WILEY VCH

RESEARCH ARTICLE

Aromaticity and Magnetic Behavior in Benzenoids: Unraveling Ring Current Combinations

Luis Leyva-Parra,[a] [b] Ricardo Pino-Ríos,[c] [d] Diego Inostroza,[a] [b] Miquel Solà,*[e] Mercedes Alonso*[f] and William Tiznado*[a]

[a] Dr. L. Leyva-Parra, Dr. D. Inostroza, Prof. W. Tiznado.
Centro de Química Teórica & Computacional (CQT&C)
Departamento de Ciencias Químicas
Facultad de Ciencias Exactas
Universidad Andrés Bello
República 275, 8370146, Santiago (Chile)
E-mail: wtiznado@unab.cl

[b] Dr. L. Leyva-Parra, Dr. D. Inostroza
Programa de Doctorado en Fisicoquímica Molecular
Facultad de Ciencias Exactas
Universidad Andrés Bello
República 275, 8370146, Santiago (Chile)

[c] Dr. R. Pino-Ríos
Instituto de Estudios de la Salud
Universidad Arturo Prat
Iquique 1100000 (Chile)

[d] Dr. R. Pino-Ríos
Química y Farmacia
Facultad de Ciencias de la Salud
Universidad Arturo Prat
Casilla 121, Iquique 1100000 (Chile)

[e] Prof. M. Solà
Institute of Computational Chemistry and Catalysis
Departament of Chemistry
University of Girona
C/M Aurélia Campmany 69, 17003, Girona, Catalonia (Spain)
E-mail: mique.sola@udg.edu

[f] Prof. M. Alonso
Departament of General Chemistry (ALGC)
Vrije Universiteit Brussel
Pleinlaan 2, 1050 Brussels (Belgium)
E-mail: Mercedes.alonso.giner@vub.be

Abstract: Nowadays, an active research topic is the connection between Clar's rule, aromaticity, and magnetic properties of polycyclic benzenoid hydrocarbons. In the present work, we employ a meticulous magnetically induced current density analysis to define the net current flowing through any cyclic circuit, connecting it to aromaticity based on the ring current concept. Our investigation reveals that the analyzed polycyclic systems display a prominent global ring current, contrasting with subdued semi-local and local ring currents. These patterns align with Clar's aromatic π-sextets only in cases where migrating π-sextet structures are invoked. The results of this study will enrich our comprehension of aromaticity and magnetic behavior in such systems, offering significant insights into coexisting ring current circuits in these systems.

Introduction

In 1931, Erich Hückel laid the foundation for the influential 4*n* + 2 rule elucidating the stability of benzene vis-à-vis cyclooctatetraene and cyclobutadiene,[1] which was firmly established by Doering and Detert in 1951,[2] The rule posits that planar (or near-planar) monocyclic molecules with (4*n* + 2) π-electrons show aromatic behavior, where *n* is a non-negative integer. The rule supports higher stability of closed-shell systems with (4*n* + 2) π-electrons. Yet, it meets challenges when applied to polycyclic systems, motivating alternative models such as Clar's π-sextet rule.

The book "The Aromatic Sextet," published in 1972, introduced Clar's rule.[3] It evolved from the foundational work of Armit and Robinson, who coined the term aromatic π-sextet in 1925.[4] According to Clar, the Kekulé resonance structure with the maximum number of disjoint aromatic π-sextets, namely benzene-like constituents, is the most significant for defining the

properties of polycyclic aromatic hydrocarbons (PAHs). Previous studies have supported the presence of resonant π-sextets in PAHs and their enhanced stability, invoking the aromaticity concept and its assessment according to different criteria such as magnetic criteria (e.g. ring current analysis, ACID, NICS, and isotropic magnetic shielding measurements),[5] energetic criteria (e.g, resonance energy, aromatic stabilization energy),[6] structural criteria (e.g. HOMA),[5i] electronic criteria (e.g. PDI, EDDB),[5i, 7] and other criteria such as simulated scanning tunneling microscope (STM) imaging[8] and HOMO-LUMO gap calculations.[9]

The relationship between Clar's rule, aromaticity, and magnetic properties has developed into an active research area, with theoretical and experimental studies offering significant insights into PAHs' electronic structure and magnetic behavior.[5f, 10] In particular, analyzing the magnetically induced current density and identifying ring currents are fundamental to interpreting aromatic species' NMR and EPR spectra.[11]

The ring current concept in antiaromatic/aromatic molecules states that molecular rings sustain a net paratropic/diatropic ring current under an external magnetic field perpendicular to the molecular ring. Non-aromatic molecules, conversely, exhibit weak or zero net ring currents, potentially due to cancellation between diatropic and paratropic ring currents of similar magnitude.[12] Although all molecules can exhibit cyclic current flows in response to external magnetic fields –whether encompassing the entire molecule or confined to localized electron regions such as lone pairs, core pairs, and bond pairs– a distinctive trait of 'aromatic' molecules is the presence of ring currents traversing through a molecular ring. More recently, ring current analysis has been expanded to three-dimensional systems or molecular architectures where not all atoms in the cyclic loop are necessarily connected by covalent bonds.[12d, 13]

In polycyclic aromatic molecules, the ring currents can be categorized as local (restricted to a single molecular ring), semi-local (encompassing more than one molecular ring), or global (covering the entire system periphery).[12d, 14] Consequently, determining the precise pathways of these currents can be challenging given the multitude of feasible scenarios.[15] The most prevalent descriptors for interpreting the ring current concept computationally are those based on magnetic shielding (e.g., NICS),[16] serving as indirect sensors of magnetically induced current densities. Previous studies suggest that contributions to NICS values of a given ring of the different circuits (local, semilocal, global) are inversely proportional to their size.[17] Additionally, some methods based on NICS have been proposed (e.g., NICS-XY-scan and NICS2BC),[19] aiming to determine the distribution of ring currents within polycyclic compounds and the effect of topology on the overall aromatic profile.

However, interpretations can diverge even when rooted in the same criterion, especially in "problematic" systems like rings incorporating heavy atoms[18] or fused rings –cases of particular interest in this study. One of the most precise methods to identify all ring currents in a polycyclic system is calculating the current strengths susceptibilities through selected chemical bonds, including common chemical bonds of annelated rings, making it possible to distinguish between local, semilocal, and global ring currents, a technique proposed by Sundholm, Berger, and Fliegl.[23] This methodology allows determining the most appropriate combination of ring current circuits within a specific system. Herein, we report a theoretical investigation by analyzing the current strength profiles to determine ring current combinations in benzenoid polycyclic systems. In addition, we highlight the method's constraints and provide recommendations for undertaking such advanced analyses.

Computational Details

The molecular structures of the different PAHs were optimized at the PBE0[24]/def2-TZVP[25] level, carried out using the Gaussian 16B.01[26] software. Assessing vibrational frequencies at the same level validates that the optimized structures correspond to true minima on their respective potential energy surfaces. The cartesian coordinates for these optimized systems are presented in the supporting information. Previous research has demonstrated the adequacy of this level of theory in obtaining reliable structures and accurate magnetic properties. This conclusion was drawn from an accuracy assessment conducted on a series of 27 small molecules.[27]

The Gauge-Including Atomic Orbital (GIAO)[28] method facilitated the calculation of the magnetically induced current densities, performed with the GIMIC[29] program at the PBE0[24]/def2-TZVP[25] level. It is important to highlight that functionals such as PBE0, when combined with suitable basis set functions, performs well in calculating magnetically induced current densities using the GIMIC program.[27, 30] For these computations, the external magnetic field was maintained along the z-axis, perpendicular to the molecular plane. Current density units are in nA/T. For qualitative analysis, we generated plots of current density vectors in viewing planes at 0.0, 0.5, and 1.0 Å above the molecular plane (Figure S1-S7). Diatropic and paratropic currents are assumed clockwise and counterclockwise, respectively. The Paraview5.10.0[31] program was used to visualize the current density paths.

Guided by a thorough examination of the plots of the current density vectors, we selected integration planes oriented perpendicularly to the molecular plane (Figures S1-S7). We placed them to pass through bonds or one or more atoms. It is essential to underscore that these planes were deliberately chosen to intersect the path of the annular current flows. Wherever feasible, they were designed to symmetrically traverse the vortices, indicative of local contributions such as core electrons or localized bonds, or to circumvent them entirely. This setup ensures a symmetrical separation of the inflow and return flows, simplifying their quantification. When avoided, it prevents the potential coupling of these vortices to the analyzed annular currents. This meticulous approach allowed us to optimize our measurements. The current strength passing through the molecule through a narrow slice of 0.05 x 5 Å is obtained by numerical integration. The integration is repeated for each slice from the bond center to a very long distance where the current density vanishes. The total length of the planes varies (see Table S1), and their height is 5.0 Å (2.5 Å above and 2.5 Å below the molecular plane). The two-dimensional Gauss-Lobatto algorithm[32] was used to integrate the currents passing through

an integration plane, and, the total current strength is obtained by summing the contributions from the slices.[12d, 29] Note that various approaches for integrating current flows have been proposed in the literature.[33] For comparative analysis, the current density in selected systems has been dissected into its σ and π contributions. This evaluation was conducted utilizing the AIMAll software, version 19.10.12.[34]

Results and Discussion

Our analysis starts with the archetypal aromatic benzene molecule. Figure 1 shows the current density vectors displayed on two different planes: at the molecular plane (σ_h) and 0.5 Å above. This figure also presents the integration planes and current strength profiles (nA/T/Å). Visualizing current density vectors in the σ_h-plane reveals different patterns of local current flows, including vortices around atomic nuclei and at chemical bonding regions. Additionally, two types of ring currents are observed. The first is a diatropic ring current, prominently in the periphery surrounding the ring formed by the six hydrogens. The second is a paratropic ring current, noticeable within the C_6 ring. Shifting the focus to a plane located 0.5 Å above, the local vortices vanish, leaving only the ring currents visible. The diatropic ring current displays maximum intensity around the C_6 ring and extends to the hydrogen atoms. The paratropic ring current remains discernible, although its intensity is somewhat diminished. In this plane, the reduction in intensity both inside the C_6 ring and around the H_6 ring aligns with the well-established notion of σ-electron delocalization defining both the diatropic region (surrounding the hydrogens) and the paratropic ring current within the C_6 ring.[35] The observed patterns of current density flux agree with numerous prior studies.[5e, 12d, 29b, 36]

The A and C planes intersect a carbon atom, yielding a thin, well-defined paratropic band aligned with the carbon atom coordinate. This band integrates to values of -1.9 and -2.1 nA/T, allowing us to assign a current strength value of 2.0 nA/T to the carbon vortex, inverting the sign because we are analyzing the return current since the direction of the vortex flow is diatropic, underscoring the principle of charge conservation as schematized in Figure 1e. A and B planes allow differentiating the paratropic ring current (circuit b in Figure 1e). In the A-plane profile, we can quantify the vortex current strength of the C-H bond (0.9 nA/T) and that of the C-C bond in the B- and C-planes (1.3 nA/T). However, in plane B, the C-C vortex contribution must be subtracted to ascertain a ring current strength (RCS) of -3.6 nA/T, which aligns with the value obtained in plane A. Once we define the local loops current strengths for the core and localized bonds and the paratropic ring current strength (b), we can devise simple equations to estimate the diatropic ring current strength (denoted as the circuit "a" in Figure 1e). According to plane A, the ring current "a" possesses a current strength of 14.8 nA/T, whereas the analysis of plane B suggests a value of 15.5 nA/T and plane C forecasts a lower value (13.3 nA/T). The reduced value in plane A might result from numerical integration errors, while the positioning of plane C –tangential to the molecular ring– could prevent part of the ring current flow from passing through it. This finding implies that a plane along a C-C bond in polycyclic systems could inherently be inaccurate in differentiating local ring currents from semi-local or global ones. It is worth noting that in the case of the diatropic circuit 'a', we have schematized it as a double cyclic current flow (Figure 1e), where the dashed lines (in light blue) delineate the flow circulating at the ring's periphery (involving the H atoms). In a different study, this current flow was characterized as a σ-type with identical magnitude but opposite in sign to the paratropic cyclic current 'b,' which is also of a σ-character.[35]Although our GIMIC analysis does not provide the capability to separate the σ-component, it is important to mention it for a more coherent interpretation relating to the current patterns manifested in the current density vector plots.

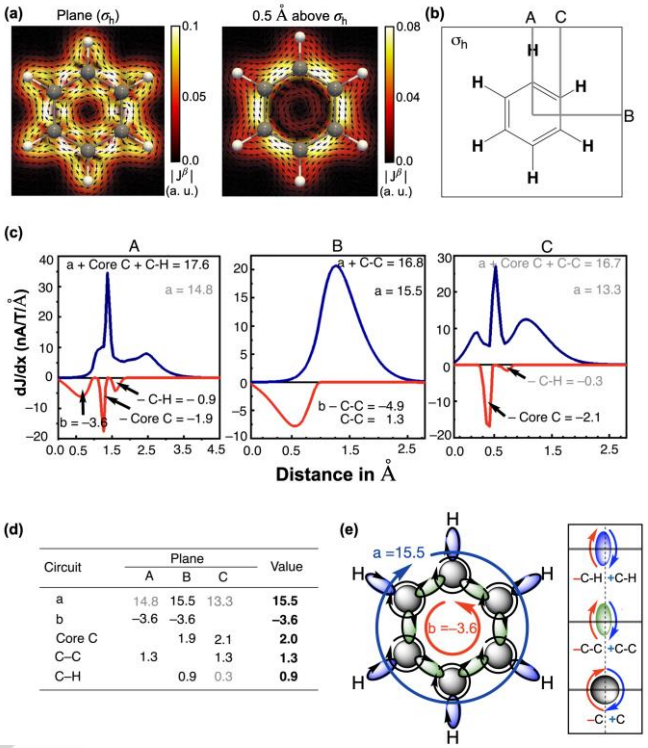

Circuit	Plane A	Plane B	Plane C	Value
a	14.8	15.5	13.3	**15.5**
b	−3.6	−3.6		**−3.6**
Core C		1.9	2.1	**2.0**
C–C	1.3		1.3	**1.3**
C–H		0.9	0.3	**0.9**

Figure 1. Results of the current density analysis of benzene: (a) Visual representation of current density vectors, current density ($|J^\beta|$) values are given in atomic units (1 a. u. = 100.63 nA/T/Å^2). (b) Integration planes. (c) Profiles of current strength (nA/T/Å), planes A-C. (d) Detected RCS for cyclic current circuits, numbers in gray, are discarded in the final calculation because they are low and may not sufficiently represent the evaluated circuit flux. (e) Schematic representation of ring currents and their respective strengths (measured in nA/T).

In light of our benzene analysis, we now focus on several important aspects when examining current strength profiles. These profiles reveal bands corresponding to specific contributions from core, bond, or ring currents. However, additional bands may emerge where these contributions coincide, enabling us to derive equations that facilitate the analysis of circuit combinations in compliance with these equations. A critical factor in formulating these equations is determining whether the current is an input or return and its tropicity characterization by qualitative analysis of the current density vector representations. To illustrate this issue, we introduce Scheme 1 which employs a hypothetical circuit combination model that merges local, semi-local, and global diatropic ring currents (in blue), incorporating paratropic ring currents within the local ones (in red). Regarding tropicity, the diatropic ring currents enter above the integration plane, as depicted in Scheme 1, while the paratropic ring currents enter below. Conversely, return currents enter on the opposite side of the plane, thus aligning with the inverse tropicity profile.

Recognition of this behavior is essential before quantitative analysis and must be considered when formulating the equations. Given that the return current must be represented with the opposite sign, a simple approach is to multiply by -1.

In the latter part of Scheme 1, we demonstrate the application of this concept to the benzene analysis previously discussed, where return currents must be accounted for in circuits associated with the core and bond vortices.

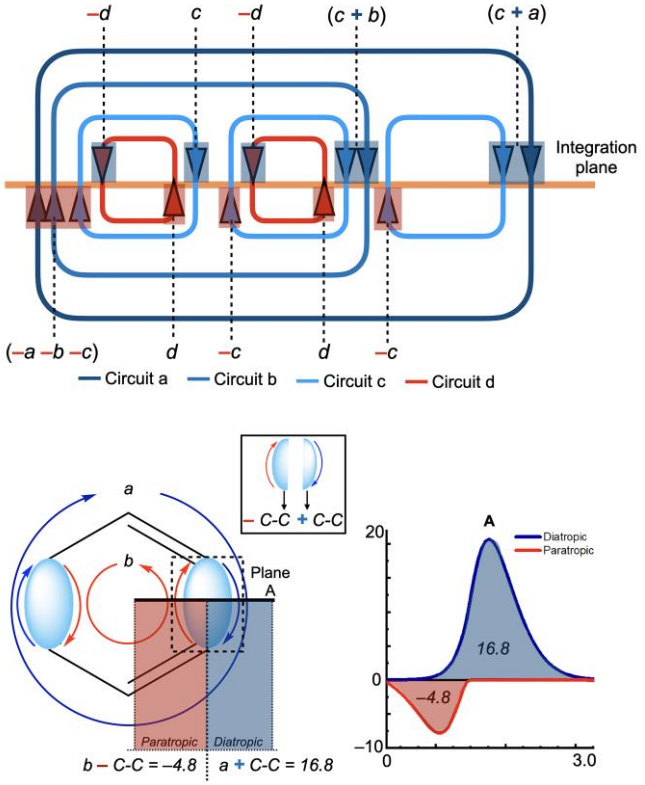

Scheme 1. This diagram illustrates local, semi-local, and global ring currents, highlighting the regions that should emerge as bands in the current strength profiles. Additionally, it presents the equations that should account for the contributions within each band, considering a specified plane of integration. The lower section of the scheme demonstrates how this strategy is applied to the analysis of benzene.

Figure 2a shows the current density of naphthalene ($C_{10}H_8$), the simplest linear acene in our study, depicted in vector plots within two planes positioned at 0.0 and 0.5 Å from the molecular plane. Local vortices, two paratropic local ring current loops nested within the benzenoid rings, and a global diatropic loop encircling the entire molecule are all discernible in plane A. This pattern also becomes evident in the plane at 0.5 Å above the molecular plane, which features a pronounced local vortex around the C-C bond linking the two benzenoid rings.

Figure 2b illustrates the selected planes (A and B), whose profiles underwent analysis to ascertain the local and global ring current strengths. Figure 2c displays the current strength profiles for each plane; their contributions are expressed either in values (nA/T) or as equations. Figure 2d unveils three hypothetical combinations (I-III) of local and global ring currents alongside their respective current strengths. These ring current combinations can be inferred through a qualitative inspection of the current density vector plots, a practice regularly utilized in this type of analysis. Yet, as demonstrated below, evaluating the profiles of current strength enables us to more precisely determine which representation or representations are most fitting through a quantitative analysis.

While Scheme I - two overlapping local diatropic ring current loops - is ruled out due to its incompatibility with the equation derived from the B-plane profiles (Figure 2c), Schemes II and III emerge as feasible, given their consistency with all possible equations (Figure 2c). Minor discrepancies may be observed in the values determined for each contribution across different equations and planes, primarily attributable to numerical integration errors.
Though Sundholm et al. originally proposed Scheme II for naphthalene,[13a] the emergence of a strengthened C-C vortex cannot be justified as there is no significant difference in the bond distance compared to other C-C bonds, nor is any induced polarization bond (e.g. by heteroatoms of different electronegativity). Scheme II was also considered by us in a previous work.[37] Therefore, we propose Scheme III as the more satisfactory model, where a global diatropic ring current (12.4 nA/T) coexists with two local diatropic ring currents of smaller intensity (3.1 nA/T) and two local paratropic ring currents within each benzenoid ring (-2.9 nA/T). This result is in agreement with a recent work, in which, based on $NICS(1)_{zz}$ values, the authors concluded that the influence of the global circuit of 10π-electrons was more important than that of the local circuit of 6π-electrons (60% vs. 40%).[7] However, calculations based on the structural index HOMA and electronic indices favored the local circuits of 6π-electrons.[7]

We can project a behavior pattern applicable to larger acenes through naphthalene analysis. This pattern includes a dominant global diatropic ring current, less intense semi-local diatropic ring currents, weaker local diatropic ring currents, and feeble paratropic ring currents within the benzene rings.

Isotropic magnetic shielding contour plots used in aromaticity analyses suggest that the local aromaticity of terminal rings decreases as the acene length increases.[10b] Moreover, these studies indicate greater aromaticity within acene's central rings than in the peripheral ones, inferring an amplified influence of migrating sextets within the inner rings, aligning with previous NICS studies.[38] Contrary to this mainstream view, our analysis, as depicted in Figure 3, paints a somewhat different picture for n-acenes (n=3-5). We discern a dominant global diatropic ring current, the strength of which diminishes as the system size enlarges. Concurrently, we detect weaker semilocal diatropic and local paratropic ring currents, accompanied by even less intense local diatropic currents. In our analysis, it is important to highlight that we have assumed the local diatropic currents to be of equivalent magnitude. This assumption is primarily based on their relatively low values and is necessary to solve the resulting equations. Moreover, any potential differences between rings are unlikely to exceed 1.0 nA/T, justifying this approximation in our analysis.

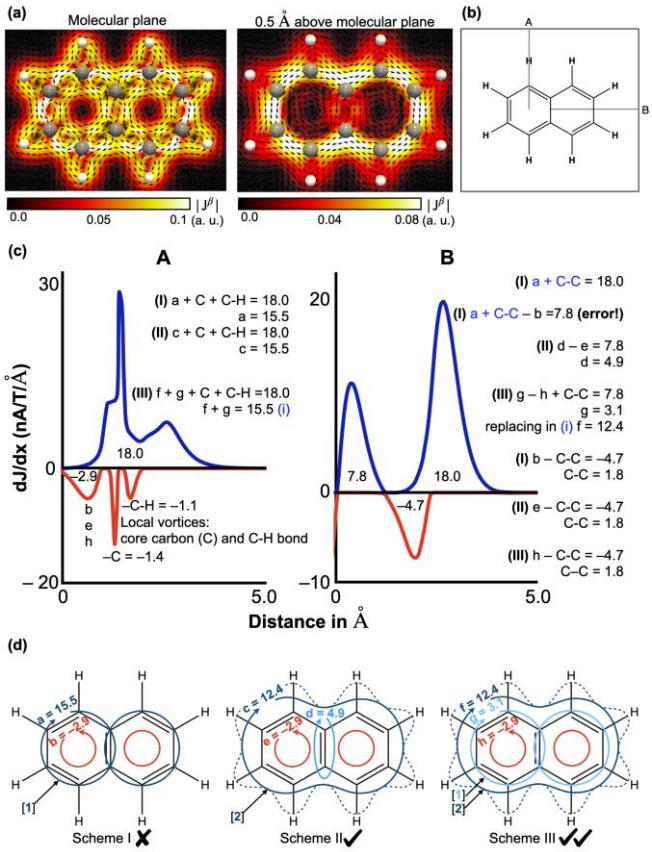

Figure 2. Results of the current density analysis for naphthalene: (a) Current density vector visualization plots. $|J^{\beta}|$ values are given in atomic units (1 a. u. = 100.63 nA/T/ Å^2). (b) Integration planes (A and B). (c) Current strength profiles corresponding to each selected plane with the assigned values to the distinct cyclic current circuits. The "**error!**" message means that this equation is inconsistent. (d) The schematic diagram of the ring currents and their measured strengths in nA/T. The number in brackets indicates the number of benzenoid rings that wrap the circuit.

This scenario partially diverges from Clar's migrating π-sextet model (Figure 3), as our ring current analysis considerably downplays the role of local benzenoid delocalizations. While our observations provide novel insights into acene aromaticity, it also supports the need to consider the adducts' aromaticity to explain the acenes' reactivity.[10d, 39]

Figure 4 depicts schematic diagrams showcasing the identified current loops and their respective strengths (measured in nA/T) within selected polycyclic aromatic hydrocarbons, namely phenanthrene, triphenylene, pyrene, and coronene. These compounds were explicitly selected to extend our comparative analysis with Clar's structures. The current strength profiles, obtained through selected planes, are used to identify the distinct cyclic circuits and their intensities, as presented in Figures S4-S7. These figures also outline the equations utilized in the analysis.

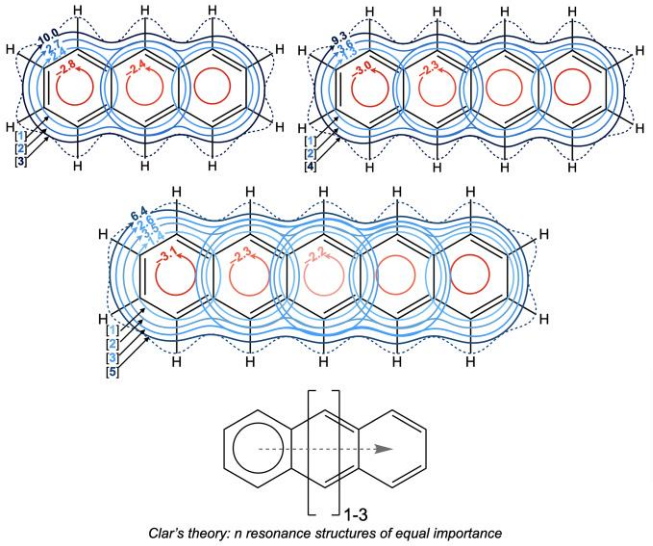

Figure 3. Schematic diagram of the identified ring currents and their measured strengths in nA/T of linear [n]acenes (n=3-5). The number in brackets indicates the number of benzenoids rings that wrap the circuit. The migrating Clar sextets are also shown.

Our analysis discerned a predominant global ring current in all the compounds. Phenanthrene showed no semilocal currents, while triphenylene and coronene exhibited semilocal currents involving an outer and central ring current circuit. Notably, triphenylene displayed intense diatropic local ring currents. A striking observation was identifying a dumbbell-shaped semilocal circuit within the structure of pyrene, underscoring the vast delocalization possibilities inherent to these polycyclic systems. The elucidation of these complex combinations is feasible only by deploying suitable methodologies. Note that for triphenylene, we have derived two representations (Figure S5). The first (Scheme 1 in Figure. S5) comprises an intense global diatropic ring current and local diatropic and paratropic ring currents. The second (Scheme 2 in Figure S5) also includes semi-local ring currents. In alignment with our previous results, we select the latter representation that considers semi-local ring currents, which is depicted in Figure 4.

While certain relationships between the Clar structures of these systems were observed, the complexity of ring current circuit combinations resists simplification. Therefore, it remains challenging, if not virtually impossible, to anticipate the nature of these currents using less sophisticated methods. This intricacy highlights the need for advanced analytical tools and methodologies to analyze magnetic behavior and its relationship with aromaticity in these systems.

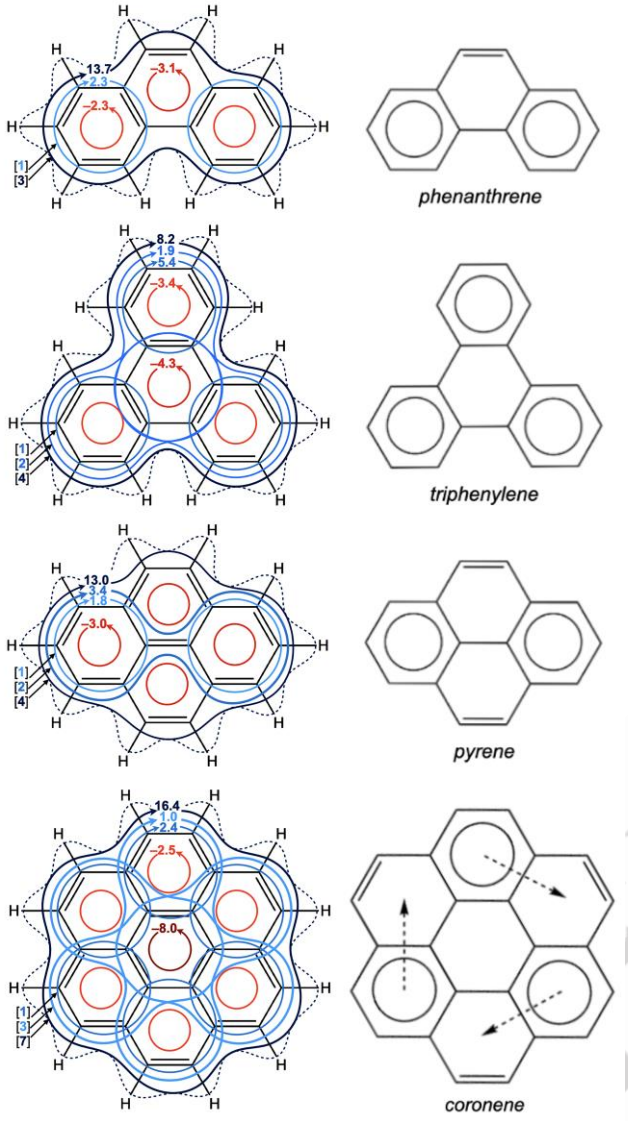

Figure 4. Schematic diagrams of the identified ring currents and their measured strengths in nA/T of selected systems. It is also shown their corresponding Clar representations. The number in brackets indicates the number of benzenoids rings that wrap the circuit.

In the peer-review process of this manuscript, a recurring point of discussion among reviewers pertains to the exclusive evaluation of the π-contribution to the current density. To address this point, we designed our analysis to elucidate the ring currents and their diatropic or paratropic nature in a series of benzenoid compounds. Our findings should align with an analysis that focuses exclusively on the π-component. Figure 5 delineates the bisected current density analysis for benzene, naphthalene, and phenanthrene to substantiate this assertion. For benzene, a total current strength of 12.2 nA/T is observed, predominantly arising from the π-component (11.8 nA/T). This result is in close agreement with our calculated net ring current value of 11.9 nA/T, obtained by subtracting the paratropic contribution (–3.6 nA/T) from the diatropic contribution (15.5 nA/T). In the context of naphthalene, the current strength analysis reveals a global current of 13.2 nA/T, primarily of π-character (12.8 nA/T). The absence of discernible local currents underscores the limitation of solely analyzing net currents traversing a bond. Specifically, the null contribution in the bond shared between the two benzenoid units could be attributed to multiple scenarios, each of which we have rigorously examined through our computational schemes. Lastly, we consistently identify a predominant global ring current across all systems studied, which is particularly intriguing when considering the reactivity of phenanthrene, which features an olefinic bond well accounted for by Clar's aromatic sextet model. However, as illustrated in Figure 5c, the ring current strengths attributable to the π-component align with our analysis.

In summary, our investigation is geared towards identifying and quantifying ring currents in a representative set of benzenoid systems. The correlation between these ring currents and the intrinsic reactivity of these systems falls outside the purview of this study.

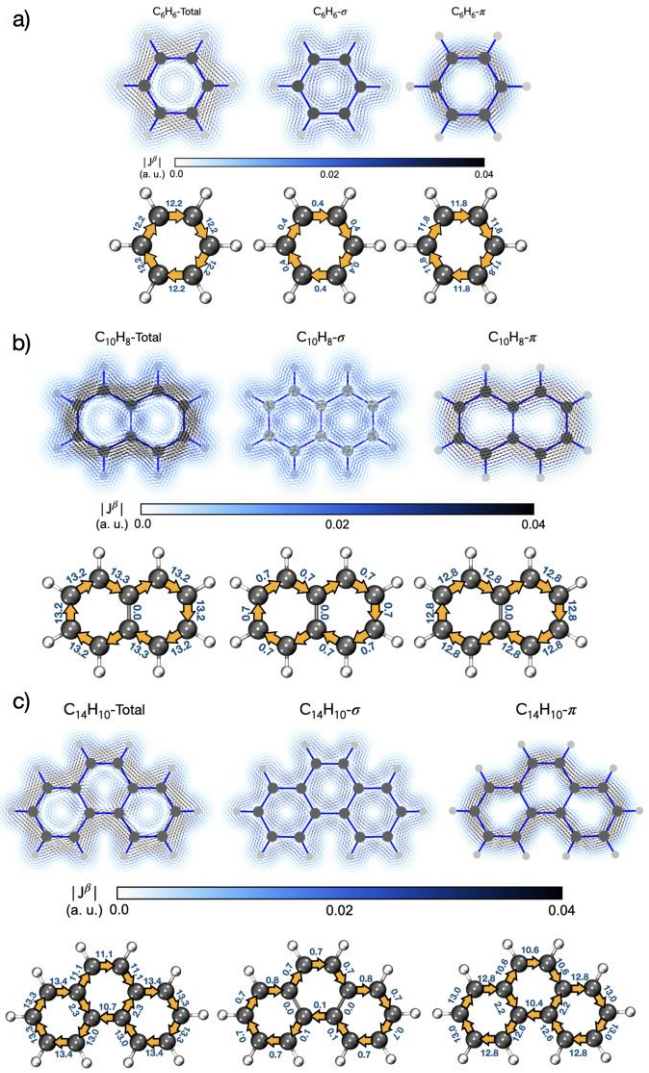

Figure 5. Vector maps of current density located 0.5 Å above the molecular plane for benzene (a), naphthalene (b), and phenanthrene (c). Corresponding current strengths in nA/T are also provided.

Conclusion

In summary, we have comprehensively analyzed the aromaticity and magnetic behavior in polycyclic benzenoid hydrocarbons. Our study reveals a prominent global ring current in these systems and subdued semi-local and local ring currents.

If we consider that π-sextets should involve only local ring currents, then the observed patterns align with Clar's aromatic π-sextets only for migrating π-sextet structures.

Acknowledgements

This work was supported by the financial support of the National Agency for Research and Development (ANID) through FONDECYT project 1211128 (W. T) and 1230571 (R. P-R). National Agency for Research and Development (ANID)/Scholarship Program/BECAS DOCTORADO NACIONAL/2020-21201177 (L. L-P). National Agency for Research and Development (ANID)/Scholarship Program/BECAS DOCTORADO NACIONAL/2019-21190427 (D. I). M.S. thanks the Spanish Ministerio de Ciencia e Innovación (project PID2020-13711GB-I00) and the Generalitat de Catalunya (project 2021SGR623). M.A. thanks the Vrije Universiteit Brussel (VUB) for financial support through a Strategic Research Program awarded to the ALGC research group. Powered@NLHPC: This research was partially supported by the supercomputing infrastructure of the NLHPC (ECM-02) and the VSC (Flemish Supercomputer Center), funded by the Research Foundation - Flanders (FWO) and the Flemish Government.

Conflict of Interest

The authors declare no conflict of interest.

Keywords: Aromaticity • Clar's aromatic π-sextets • Polycyclic benzenoid hydrocarbons • Ring Currents

[1] a) E. Hückel, *Z. Phys.* **1931**, *72*, p. 310-337; b) E. Hückel, *Z. Phys.* **1931**, *70*, p. 104-186; c) E. Hückel, *Z. Phys.* **1932**, *76*, p. 628-648; d) E. Hückel, *Z. Elektrochem.* **1937**, *43*, p. 752-788; p. 827-849.

[2] W. von E. Doering, F. L. Detert, *J. Am. Chem. Soc.* **1951**, *73*, 876-877.

[3] E. Clar in *The Aromatic Sextet.* Wiley, New York, **1972**.

[4] T. W. Armit, R. Robinson, *J. Chem. Soc. Trans* **1925**, *127*, 1604-1618.

[5] a) E. Steiner, P. W. Fowler, *Int. J. Quantum Chem.* **1996**, *60*, 609-616; b) Y. Anusooya, A. Chakrabarti, S. K. Pati, S. Ramasesha, *Int. J. Quantum Chem.* **1998**, *70*, 503-513; c) A. Ligabue, U. Pincelli, P. Lazzeretti, R. Zanasi, *J. Am. Chem. Soc* **1999**, *121*, 5513-5518; d) E. Steiner, P. W. Fowler, L. W. Jenneskens, *Angew. Chem. Int. Ed.* **2001**, *40*, 362-366; e) E. Steiner, P. W. Fowler, R. W. A. Havenith, *J. Phys. Chem. A* **2002**, *106*, 7048-7056; f) E. Steiner, P. W. Fowler, A. Soncini, L. W. Jenneskens, *Faraday Discuss.* **2007**, *135*, 309-323; g) D. Sundholm, R. J. Berger, H. Fliegl, *Phys. Chem. Chem. Phys.* **2016**, *18*, 15934-15942; h) D. Geuenich, K. Hess, F. Köhler, R. Herges, *Chem. Rev.* **2005**, *105*, 3758-3772; i) G. Portella, J. Poater, M. Solà, *J. Phys. Org. Chem.* **2005**, *18*, 785-791; j) P. B. Karadakov, B. VanVeller, *Chem. Commun.* **2021**, *57*, 9504-9513; k) B. J. Lampkin, P. B. Karadakov, B. VanVeller, *Angew. Chem. Int. Ed.* **2020**, *59*, 19275-19281.

[6] J. Aihara, *J. Phys. Chem. A* **2003**, *107*, 11553-11557.

[7] D. W. Szczepanik, M. Solà, T. M. Krygowski, H. Szatylowicz, M. Andrzejak, B. Pawelek, J. Dominikowska, M. Kukulka, K. Dyduch, *Phys. Chem. Chem. Phys.* **2018**, *20*, 13430-13436.

[8] T. Wassmann, A. P. Seitsonen, A. M. Saitta, M. Lazzeri, F. Mauri, *J. Am. Chem. Soc.* **2010**, *132*, 3440-3451.

[9] Y. Ruiz-Morales, *J. Phys. Chem. A* **2004**, *108*, 10873-10896.

[10] a) P. B. Karadakov and B. VanVeller, *Chem. Commun.* **2021**, *57*, 9504-9513; b) B. J. Lampkin, P. B. Karadakov, B. VanVeller, *Angew. Chem. Int. Ed.* **2020**, *132*, 19437-19443; c) F. Alvarez-Ramírez, Y. Ruiz-Morales, *J. Chem. Inf. Model.* **2019**, *60*, 611-620; d) M. Solà, *Front. Chem.* **2013**, 22; e) Y. Ruiz-Morales, *J. Phys. Chem. A* **2004**, *108*, 10873-10896.

[11] a) A. V. McBeath, R. J. Smernik, M. P. Schneider, M. W. Schmidt, E. L. Plant, *Org. Geochem.* **2011**, *42*, 1194-1202; b) R. H. Mitchell, *Chem. Rev.* **2001**, *101*, 1301-1315.

[12] a) P. Lazzeretti, *Progress in Nuclear Magnetic Resonance Spectroscopy* **2000**, *36*; b) R. McWeeny, *Mol. Phys.* **1958**, *1*, 311-321; c) J. A. Pople, *Mol. Phys* **1958**, *1*, 175-180; d) D. Sundholm, H. Fliegl, R. J. Berger, *WIREs Comput. Mol. Sci.* **2016**, *6*, 639-678.

[13] a) I. Fernández, *Aromaticity: Modern Computational Methods and Applications*, Elsevier, **2021**, p; b) R. Pino-Rios, A. Vásquez-Espinal, O. Yañez, W. Tiznado, *RSC Adv.* **2020**, *10*, 29705-29711.

[14] J. Aihara, *J. Am. Chem. Soc.* **2006**, *128*, 2873-2879.

[15] S. Escayola, A. Poater, A. Muñoz-Castro, M. Solà, *Chem. Commun. (Camb)* **2021**, *57*, 3087-3090.

[16] P. v. R. Schleyer, C. Maerker, A. Dransfeld, H. Jiao, N. J. van Eikema Hommes, *J. Am. Chem. Soc.* **1996**, *118*, 6317-6318.

[17] S. Fias, S. Van Damme, P. Bultinck, *J. Comp. Chem.* **2008**, *29*, 358-366.

[18] a) C. Foroutan-Nejad, *Theory. Chem. Acc.* **2015**, *134*, 1-9; b) J. J. Torres-Vega, A. Vásquez-Espinal, J. Caballero, M. L. Valenzuela, L. Alvarez-Thon, E. Osorio, W. Tiznado, *Inorg. Chem.* **2014**, *53*, 3579-3585; c) W. Rabanal-León, A. Vásquez-Espinal, O. Yañez, R. Pino-Rios, R. Arratia-Pérez, L. Alvarez-Thon, J. Torres-Vega, W. Tiznado, *Eur. J. Inorg. Chem.* **2018**; d) A. Vásquez-Espinal, R. Pino-Rios, L. Alvarez-Thon, W. A. Rabanal-León, J. J. Torres-Vega, R. Arratia-Perez, W. Tiznado, *J. Phys. Chem. Lett.* **2015**, *6*, 4326-4330.

[19] a) R. Gershoni-Poranne, A. Stanger, *Chem. Eur. J.* **2014**, *20*, 5673-5688; b) R. Gershoni-Poranne, *Chem. Eur. J.* **2018**, *24*, 4165-4172; c) E. Paenurk, R. Gershoni-Poranne, *Phys. Chem. Chem. Phys.* **2022**, *24*, 8631-8644.

[20] A. Rehaman, A. Datta, S. S. Mallajosyula, S. K. Pati, *J. Chem. Theory Comput.* **2006**, *2*, 30-36.

[21] Y.-C. Lin, D. Sundholm, J. Jusélius, *J. Chem. Theory Comput.* **2006**, *2*, 761-764.

[22] J. Cao, G. London, O. Dumele, M. von Wantoch Rekowski, N. Trapp, L. Ruhlmann, C. Boudon, A. Stanger, F. Diederich, *J. Am. Chem. Soc.* **2015**, *137*, 7178-7188.

[23] D. Sundholm, R. J. Berger, H. Fliegl, *Phys. Chem. Chem. Phys.* **2016**, *18*, 15934-15942.

[24] C. Adamo, V. Barone, *J. Chem. Phys.* **1999**, *110*, 6158-6170.

[25] F. Weigend, R. Ahlrichs, *Phys. Chem. Chem. Phys.* **2005**, *7*, 3297-3305.

[26] M. J. Frisch in *Gaussian 16*, Gaussian, Inc, Wallingford CT, **2016**.

[27] S. Lehtola, M. Dimitrova, H. Fliegl, D. Sundholm, *J. Chem. Theory Comput.* **2021**, *17*, 1457-1468.

[28] K. Wolinski, J. F. Hinton, P. Pulay, *J. Am. Chem. Soc.* **1990**, *112*, 8251-8260.

[29] a) H. Fliegl, S. Taubert, O. Lehtonen, D. Sundholm, *Phys. Chem. Chem. Phys.* **2011**, *13*, 20500-20518; b) J. Juselius, D. Sundholm and J. Gauss, *J. Chem. Phys.* **2004**, *121*, 3952-3963.

[30] D. Inostroza, V. García, O. Yañez, J. J. Torres-Vega, A. Vásquez-Espinal, R. Pino-Rios, R. Báez-Grez, W. Tiznado, *New J. Chem.* **2021**, *45*, 8345-8351.

[31] U. Ayachit, *The ParaView Guide: A Parallel Visualization Application*, Kitware, Inc., USA, **2015**, p.

[32] M. Abramowitz in *Handbook of Mathematical Functions, with Formulas, Graphs, and Mathematical Tables*, New York, NY, USA, **1974**.

[33] a) S. Pelloni, P. Lazzeretti, R. Zanasi, *Theor. Chem. Acc.* **2009**, *123*, 353-364; b) S. Pelloni, F. Faglioni, R. Zanasi, P. Lazzeretti, *Phys. Rev. A* **2006**, *74*, 012506; c) P. Lazzeretti, *Phys. Chem. Chem. Phys.* **2016**, *18*, 11765-11771; d) T. A. Keith, R. F. Bader, *J. Chem. Phys.* **1993**, *99*, 3669-3682; e) T. J. Irons, L. Spence, G. David, B. T. Speake, T. Helgaker, A. M. Teale, *J. Phys. Chem. A* **2020**, *124*, 1321-1333.

[34] K. T. AIMAll 19.10.12 in *TK Gristmill Software*, *Vol.* **2019**.

[35] G. Monaco, R. Zanasi, S. Pelloni, P. Lazzeretti, *J. Chem. Theory Comput.* **2010**, *6*, 3343-3351.

[36] a) J. A. N. F. Gomes, R. B. Mallion, *Chem. Rev.* **2001**, *101*, 1349-1383; b) R. Gershoni-Poranne, A. Stanger, *Chem. Soc. Rev.* **2015**, *44*, 6597-6615.

[37] D. Inostroza, V. García, O. Yañez, J. J. Torres-Vega, A. Vásquez-Espinal, R. Pino-Rios, R. Báez-Grez, W. Tiznado, *New J. Chem.* **2021**, *45*, 8345-8351.

[38] a) J. Poater, J. M. Bofill, P. Alemany, M. Solà, *J. Phys. Chem. A* **2005**, *109*, 10629-10632; b) P. v. R. Schleyer, M. Manoharan, H. Jiao, F. Stahl, *Org. Lett.* **2001**, *3*, 3643-3646.

[39] a) P. Bultinck, *Faraday Discuss.* **2007**, *135*, 347-365; b) P. v. R. Schleyer, M. Manoharan, H. Jiao, F. Stahl, *Org. Lett.* **2001**, *3*, 3643-3646.

Entry for the Table of Contents

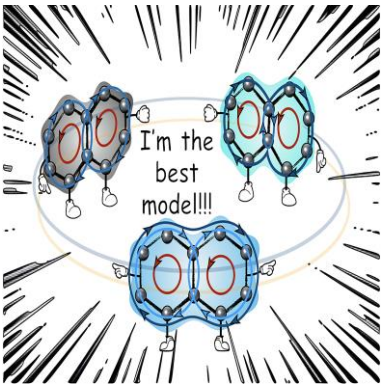

Unraveling the mysteries of ring current combinations in polycyclic benzenoid hydrocarbons.

Institute and/or researcher Twitter usernames: @ctcgunab, @leyvaluis177, @DiegoEstevan_IM, @miquelsola.